Diffusion and Drift of Charge Carriers in Molecularly Doped Polymers

Akiko Hirao, Hideyuki Nishizawa, and Masami Sugiuchi
Materials and Devices Research Laboratory, Research and Development Center, Toshiba Corporation, 1 Komukai, Toshiba-cho, Saiwai-ku, Kawasaki 210, Japan
(Received 23 January 1995)

The diffusion coefficient (D) and drift mobility (μ) of molecularly doped polymers have been obtained by Monte Carlo parameter fitting of a theoretical equation to time-of-flight transient photocurrent signals. The logarithm of μ increased linearly with $\sqrt{E}$. The negative field dependence of the mobility that has been observed at low electric field appeared to a superimposition of drift and diffusion. An anomalous field-assisted D was observed. The logarithm of D decreased linearly with T^{-2}.

PACS numbers: 66.30.Dn, 72.40.+w

Charge-transporting molecularly doped polymers (MDP's) form a system in which a carrier hops between molecules. MDP are widely used as transport layers for organic photoreceptors [1,2]. Recently, MDP have attracted attention as white light emitting organic electroluminescent devices [3], photorefractive devices [4,5], and synapse bond devices [6].

The operation of these devices depends on the characteristics of carrier transport; hence carrier transport in MDP has been the subject of numerous investigations [1,2,7–10]. Although the transport of carriers is expressed by drift and diffusion, the diffusion coefficient (D) has not been discussed because D is difficult to measure directly.

In an ordinary crystalline semiconductor, Einstein's law relating carrier mobility to diffusivity holds. Therefore, the diffusivity in the crystalline semiconductor can be determined from the mobilities [11]. Einstein's law cannot, however, be applied to a MDP that is a nonequivalent and amorphous system because organic molecules essentially retain their identity, interacting only weakly through van der Waals forces [12,13]. Therefore the D of the MDP needs to be measured individually.

In the case of nondispersive charge transport, the transient photocurrent of the time-of-flight (TOF) measurement [14] has a rectangular shape. Mobilities have been determined from transit times derived from the intersection of the asymptotes to the plateau and the trailing edge of the transients [14]. However, the decay of an actual experimental photocurrent does not have a rectangular shape. The spread of carrier packet and arrival time changes the shape of the signal [15]. Although the drift mobilities obtained from the intersection of the asymptotes have been examined [1,2,16], the transit time of mean drift mobilities cannot be defined as shoulders in transient current signals.

In order to determine the drift mobility and D, we analyzed the current signal [17–19]. In this Letter, we first introduce an equation for the shape of the transient photocurrent. Then, Monte Carlo fitting of the theoretical equation to experimental signals is used to extract the drift mobilities and the diffusion coefficients.

A sample of thickness (d) and dielectric constant (ε) is sandwiched by blocking contact metallic electrodes. The semitransparent top electrode at the position $x = 0$ is connected to a steady source of potential. The counterelectrode at the position $x = d$ is returned to ground through a resistor that is sufficiently small. Because the area of the electrode is sufficiently larger than d, the electric field vector points in the x direction. Holes of charge q and electrons of charge $-q$ are generated by pulse excitation at the position $x = 0$ and the time $t = 0$. Maxwell's equation in the x direction is

$$\frac{dE}{dx} = \frac{Q - q}{\varepsilon}\,\delta(x) + \frac{-Q}{\varepsilon}\,\delta(x - d) + \frac{\rho(x)}{\varepsilon}, \quad (1)$$

where Q is the charge on a pair of electrodes of the sample, and $\rho(x)$ is the charge density distribution of the holes. The boundary conditions applicable to the solution of Eq. (1) are $E = 0$ at $x \leqq 0$, and $E = 0$ at $x \geqq d$ because the electrodes are metal. Therefore the potential Φ is given by

$$\phi = \int_0^d E\,dx = \frac{Q - q}{\varepsilon}\,d + \frac{1}{\varepsilon}\int_0^d dx \int_0^x \rho(s)\,ds\,. \quad (2)$$

When the time constant of the external circuit is sufficiently smaller than the transit time of the hole, Φ equals the constant voltage (V). Hence the current (J) is given by

$$J = \frac{dQ}{dt} = -\frac{1}{d}\int_0^d dx \int_0^x \rho(s)\,ds\,. \quad (3)$$

We assume that the carrier distribution (n) is given by

$$n = \frac{n_0}{\sqrt{4\pi Dt}}\exp\left\{-\frac{(x - vt)^2}{4Dt}\right\}, \quad (4)$$

where v is the drift velocity and n_0 is the number of holes [20]. The holes that arrive at the counterelectrode cannot move, because they strongly combine with the electrons at

the counterelectrode. In addition to this, the hole cannot diffuse across the top electrode. Hence

$$\rho(x) = en(x) + e\int_{-\infty}^{0} n(s)\,ds\,\delta(x) + e\int_{d}^{\infty} n(s)\,ds\,\delta(x-d). \quad (5)$$

Using Eqs. (3), (4), and (5), we obtain

$$J = \frac{eD}{d}\frac{n_0}{\sqrt{4\pi Dt}}\left(\exp\left\{-\frac{(d-vt)^2}{4Dt}\right\} - \exp\left\{-\frac{(vt)^2}{4Dt}\right\}\right) - \frac{ev}{d}\frac{n_0}{2}\left(\operatorname{erf}\left\{\frac{vt}{\sqrt{4Dt}}\right\} + \text{Flag}\operatorname{erf}\left\{\frac{d-vt}{\sqrt{4Dt}}\right\}\right),$$

$$\text{Flag} = \begin{cases} 1, & d \geq vt, \\ -1, & d \leq vt, \end{cases} \quad (6)$$

where $\operatorname{erf}(x)$ represents the error function [21]. Monte Carlo parameter fitting [22] of Eq. (6) to experimental signals gives v and D.

We used this procedure to analyze carrier transport in hydrazone-doped bisphenol-A-polycarbonate. The doping concentration of 4-dibenzylamino-2-methylbenzaldehyde-1,1-diphenyl-hydrazone (BMH) in the samples was 50% by weight. The measurements were made by conventional TOF techniques [9]. The 5.4 μm MDP was sandwiched between a semitransparent Al-coated quartz glass substrate and a Au electrode. A sample of the sandwich structure was connected in a circuit with a voltage source and a resistance (R). The MDP were excited through the aluminum electrode by a 0.9 ns pulse nitrogen laser pulse (NDC, JS-1200). The penetration depth is sufficiently small compared with the thickness of the MDP. The energy per pulse incident on the MDP was adjusted such that the maximum charge generation in the MDP was less than $0.03C_sV$ where C_s is the capacitance of the sample. The transit times were 1000 times larger than the time constant of the external circuit C_sR. Over the range of fields and temperatures investigated, the mobilities were reversible, with no signs of hysteresis.

Figure 1(a) shows the typical features of an experimental transient photocurrent (solid line) and fitting result (broken line). We have succeeded in obtaining excellent fitting results for the experimental data over temperature ranges from 260 to 350 K, and over electric field ranges from 1 to 36 MV/cm. We found that Eq. (6) was consistent with the experimental signal, except for the tail of the signal. In the region of the signal tail, experimental data were higher than theoretical data. This difference could be attributed to the detrapping of the carrier from deep traps, because the density of states (DOS) profile is broad [1,7] and the carriers in the higher portion of the DOS should act as the deep traps [8]. We conclude that the transient photocurrent in the MDP can be described by Eq. (6).

The drift velocity (v) obtained by the fitting gives the transit time ($t_a = v/d$). The time t_a was not equal to the time derived from the intersection of asymptotes to the plateau and the trailing edge of the transient photocurrent

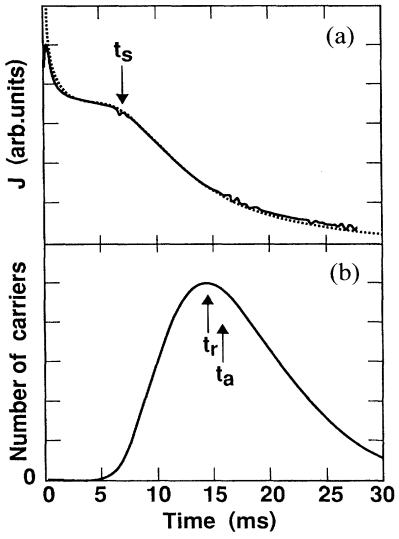

FIG. 1. (a) Time-of-flight transient photocurrent signal. The solid line is the experimentally measured photocurrent, and the broken line is the current obtained by fitting the parameters of Eq. (6) to the experimental data. (b) Time dependence of the number of arriving carriers at the counter electrode. The numbers were calculated from Eq. (5).

(t_s) and the time for which the number of arriving carriers at the counterelectrode was maximum (t_r) as shown in Fig. 1(b), where the number of arriving carriers at the counterelectrode was calculated from Eq. (5). Assuming that D is zero, t_s and t_r are equal to t_a. The time t_s is the arrival time of the earliest carriers at the counterelectrode. The earliest carriers should be transported by the superimposition of drift and forward diffusion.

The electric field dependence of the mobilities from t_s and t_a are shown in Fig. 2. The logarithm of the mobility (μ_a) calculated from t_a increased linearly with $\sqrt{E}$. The electric field dependence of $\ln\mu_s$ calculated from t_s was similar to that of $\ln\mu_a$, except for a negative field dependence in the low electric field region. This negative field dependence could be attributed to the contribution of diffusion of carriers in the low electric field. The negative field dependence of μ_s in a low electric field has been reported by Borsenberger *et al.* [23] and Young and Pule [24]. The analysis of the electric field dependence of μ_a should be much more significant than that of μ_s because μ_a does not contain the factor of diffusion.

Figure 3 shows the electric field dependence of D. This means that the diffusion is assisted by the electric field. Field-assisted (biased) diffusion has been reported from simulation of the disorder model [15].

To separate the various dependencies of μ, Schein, Rosenberg, and Rice have developed a deconvolution analysis [25]. We have analyzed the electric field and the temperature (T) dependence of D using their method.

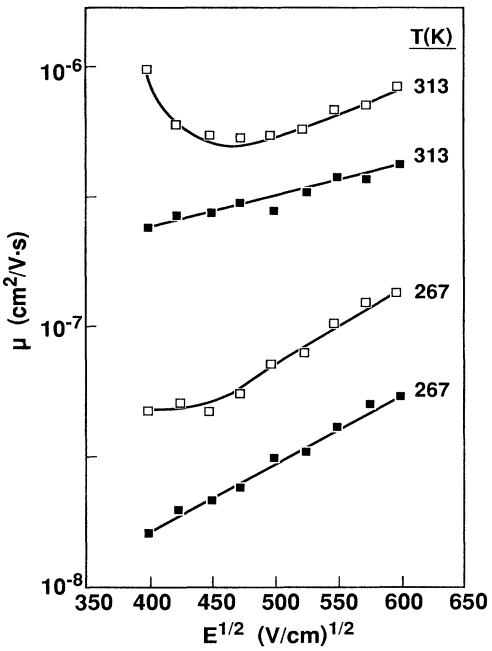

FIG. 2. Square root of the applied electric field, $\sqrt{E}$, vs the logarithm of the mobility. □ is the mobility μ_s obtained from the transit time defined as the time at which the asymptotes to the plateau and tail of the photocurrent profile intersect. ■ is the true mobility μ_a obtained by fitting the parameters of Eq. (6) to the experimental signal.

The analysis was based on the assumption that D could be described by the empirical relations

$$D(T,E) = D_0 \exp f_1(T) \exp f_2(E,T), \quad (7)$$

where D_0 is the prefactor diffusion coefficient. Provided that $f_2 \rightarrow 0$ as $E \rightarrow 0$, the temperature dependence associated with f_1 can be determined from the temperature dependence of the zero-field D. Since the logarithm of D increased linearly with $\sqrt{E}$ as shown in Fig. 3, we can describe $f_2(E,T) = S(T)\sqrt{E}$, where $S(T) = \partial \ln D/\partial\sqrt{E}$. We found a temperature dependence of zero-field diffusion that followed a $\ln D \propto T^{-2}$ relationship. Consequently,

$$f_1 = -(T_1/T)^2, \quad (8)$$

where T_1 is a constant. $S(T)$ was proportional to T^{-2}. Therefore the data can be described as

$$f_2 = C_d\{(T_1/T)^2 - \Delta\}\sqrt{E}, \quad (9)$$

where C_d and Δ are constants. Combining Eqs. (7), (8), and (9) then gives

$$D(T,E) = D_0 \exp\left[-\left(\frac{T_1}{T}\right)^2\right] \times \exp\left[C_d\left\{\left(\frac{T_1}{T}\right)^2 - \Delta\right\}\sqrt{E}\right]. \quad (10)$$

From the slope and the intercept of the $\ln D$ vs T^{-2} plot, the values of T_1 and D_0 were determined as $T_1 = 919$ K and $D_0 = 6.1 \times 10^{-3}$ cm^2/s. Furthermore, from the slope and the intercept of the S vs T^{-2} plot, the values of C_d and Δ were determined as $C_d = 1.2 \times 10^{-3}$ (cm/V)$^{1/2}$ and $\Delta = 3.7$.

Equation (10) is similar to the equation for the drift mobility by the disorder formalism [7]

$$\mu(T,E) = \mu_0 \exp\left[-\left(\frac{2\sigma}{3kT}\right)^2\right] \times \exp\left[C\left\{\left(\frac{\sigma}{kT}\right)^2 - \Sigma^2\right\}\sqrt{E}\right], \quad (11)$$

where σ is the width of the DOS, Σ is a parameter that describes the degree of positional disorder, μ_0 is the prefactor mobility, and C is an empirical constant. The results of this study showed that μ_a can be described by Eq. (11). From the experimental results, the parameters were determined as $\mu_0 = 6.1 \times 10^{-3}$ cm^2/V s, $\sigma = 0.13$ eV, $\Sigma = 4.0$, and $C = 3.3 \times 10^{-4}$ (cm/V)$^{1/2}$. The value of C was roughly the same as the theoretical value obtained by Bässler *et al.* Therefore μ_a was described by the disorder formalism.

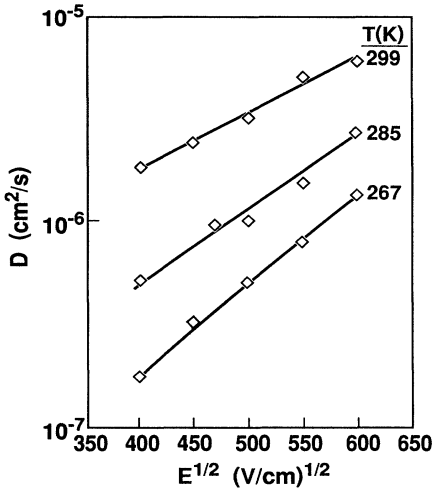

FIG. 3. Applied electric field dependence of the diffusion coefficient D.

Figure 4 shows that $\ln\mu_a$ was proportional to $\ln D$ at constant temperature. This result agrees with the result obtained by combining Eqs. (10) and (11). Since the slope of $\ln\mu_a$ vs $\ln D$, γ, is greater than 1 in Fig. 4, D increased with the electric field much more than μ_a. Richert, Pautmeier, and Bässler have reported that D increased with the electric field much more rapidly than the mobility from a simulation [13]. The experimental results matched their simulation results.

Finally, we present an explanation of the negative field dependence of μ_s at low electric field. The time t_s is that for arrival of the earliest carriers that migrate by the superimposition of drift and forward diffusion. Therefore the following relationship is obtained:

$$d = \mu_a E t_s + \alpha\sqrt{D t_s}, \quad (12)$$

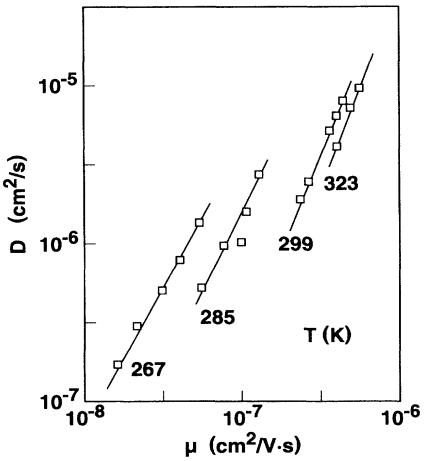

FIG. 4. Relationship between drift mobilities, μ_a, and diffusion coefficients, D.

where d is the sample thickness and α is a constant. $\alpha\sqrt{Dt_s}$ is the distance between the center of the carrier packet and the edge of the carrier packet. Using Eqs. (10) and (11), the E slope of μ_s $[= d/(t_s E)]$ is given by

$$\frac{\partial \ln \mu_s}{\partial \sqrt{E}} = \frac{\partial \ln \mu_d}{\partial \sqrt{E}} + \frac{1}{1 - PG}\left(G + \frac{1}{G + 1}\right) \times \frac{D}{2d\mu_a E}\left\{\frac{1}{T^2}\left(C_d T_1^2 - \frac{\sigma^2}{k^2}\right) - (C_d \Delta - C\Sigma^2) - \frac{2}{\sqrt{E}}\right\}, \quad (13)$$

where $P = \alpha^2 D/(2\mu_a E d)$, $G = \sqrt{2P + 1} - 1$, and usually $0 < P \ll 1$. Since $G > 0$, $\partial \ln \mu_s / \partial \sqrt{E}$ is negative at low electric field. Hence the negative field dependence of μ_s at low electric field is observed because of the contribution of carrier diffusion.

Equation (11) of the disorder formalism indicates that the mobilities decrease with increasing field at low fields and high temperature. This is caused by the increase of the number of traps that are due to off-diagonal disorder (electric field induced trap) [7]. However, the negative field dependence of μ_s at low electric fields and low temperature cannot be explained by the disorder formalism.

In conclusion, we have shown the successful fitting of the transport equation to the experimental transient current signal. We obtained drift mobilities and diffusion coefficients simultaneously by fitting. The logarithm of the drift mobility increased linearly with the square root of the applied electric field. We found that the negative field dependence of the mobility obtained from the intersection time of asymptotes of the plateau and the trailing edge of the transient photocurrent at low electric field appeared to be due to the superimposition of drift and diffusion. We also observed anomalous field-assisted diffusion. The diffusion coefficients showed the following relationship: $D(T, E) = D_0 \exp[-(T_1/T)^2] \exp[C_d\{(T_1/T)^2 - \Delta\}\sqrt{E}]$. The logarithm of the diffusion coefficients was proportional to the logarithm of the mobilities at constant temperature, and the slope was not equal to 1 ($D \propto \mu^\gamma, \gamma > 1$). These experimental results agreed with the simulation results [23].

[1] P. M. Borsenberger and D. S. Weiss, *Organic Photoreceptor for Imaging Systems* (Dekker, New York, 1993).
[2] L. B. Schein, *Electrography and Development Physics* (Springer, New York, 1992), 2nd ed.
[3] J. Kido, K. Hongawa, K. Okuyama, and K. Nagai, Appl. Phys. Lett. **64**, 815 (1994).
[4] S. Ducharme, J. C. Scott, R. J. Twieg, and W. E. Moerner, Phys. Rev. Lett. **66**, 1846 (1991).
[5] W. E. Moerner and S. M. Silence, Chem. Rev. **94**, 127 (1994).
[6] H. Körner and G. Mahler, Phys. Rev. B **48**, 2335 (1993).
[7] H. Bässler, Phys. Status Solidi (b) **175**, 15 (1993).
[8] M. Sugiuchi and H. Nishizawa, J. Imag. Sci. Technol. **37**, 245 (1993).
[9] A. Hirao, H. Nishizawa, and M. Sugiuchi, J. Appl. Phys. **74**, 1083 (1993).
[10] S. V. Novikov and A. V. Vannikov, Chem. Phys. Lett. **182**, 598 (1991).
[11] R. Kubo, M. Toda, and N. Hashitsume, *Statistical Physics II* (Springer-Verlag, Berlin, 1991), 2nd ed., p. 178.
[12] E. A. Silinsh, *Organic Molecular Crystals* (Springer-Verlag, Berlin, 1980), p. 36.
[13] R. Richert, L. Pautmeier, and H. Bässler, Phys. Rev. Lett. **63**, 547 (1989).
[14] R. C. Enck and G. Pfister, in *Photoconductivity and Related Phenomena,* edited by J. Mort and D. M. Pai (Elsevier, New York, 1976), Chap. 7.
[15] L. Pautmeier, R. Richert, and H. Bässler, Philos. Mag. B **63**, 587 (1991).
[16] A. Hirao, H. Nishizawa, and M. Hosoya, Jpn. J. Appl. Phys. **33**, 1944 (1994).
[17] P. M. Bosenberger, L. T. Pautmeier, and H. Bässler, Phys. Rev. B **48**, 3066 (1993).
[18] J. C. Scott, L. T. Pautmeier, and L. B. Schein, Phys. Rev. B **46**, 8603 (1992).
[19] J. P. Bouchaud and A. Georges, Phys. Rev. Lett. **63**, 2692 (1989).
[20] S. M. Sze, *Physics of Semiconductor Devices* (John Wiley & Sons, New York, 1981), p. 55.
[21] *Handbook of Mathematical Functions,* edited by M. Abramovitz and I. A. Stegun (Dover Publications, New York, 1970).
[22] W. H. Press, B. P. Flannery, S. A. Teukolsky, and W. T. Vetterling, *Numerical Recipes in C* (Cambridge University Press, Cambridge, 1988), p. 548.
[23] P. M. Borsenberger, E. H. Magin, M. van der Auweraer, and F. C. de Schryver, Phys. Status Solidi (a) **140**, 9 (1993).
[24] R. H. Young and N. G. Pule, Phys. Rev. Lett. **72**, 388 (1994).
[25] L. B. Schein, A. Rosenberg, and S. L. Rice, J. Appl. Phys. **60**, 4287 (1986).